

Dilepton production in proton-proton collisions at BEVALAC energies

Amand Faessler[†], Christian Fuchs^{‡§},
 Mikhail Krivoruchenko^{†‡} and Boris Martemyanov^{†‡}

[†] Institut für Theoretische Physik, Universität Tübingen
 Auf der Morgenstelle 14, D-72076 Tübingen, Germany
[‡] Institute for Theoretical and Experimental Physics
 B. Cheremushkinskaya 25, 117259 Moscow, Russia

Abstract. The dilepton production in elementary $pp \rightarrow e^+e^-X$ reactions at BEVALAC energies $T_{lab} = 1 \div 5$ GeV is investigated. The calculations include direct e^+e^- decays of the vector mesons ρ^0 , ω , and ϕ , Dalitz decays of the π^0 -, η -, ρ -, ω -, and ϕ -mesons, and of the baryon resonances $\Delta(1232)$, $N(1520)$, The subthreshold vector meson production cross sections in pp collisions are treated in a way sufficient to avoid double counting with the inclusive vector meson production. The vector meson dominance model for the transition form factors of the resonance Dalitz decays $R \rightarrow e^+e^-N$ is used in an extended form to ensure correct asymptotics which are in agreement with the quark counting rules. Such a modification gives an unified and consistent description of both $R \rightarrow N\gamma$ radiative decays and $R \rightarrow N\rho(\omega)$ meson decays. The effect of multiple pion production on the experimental efficiency for the detection of the dilepton pairs is studied. We find the dilepton yield in reasonable agreement with the experimental data for the set of intermediate energies whereas at the highest energy $T_{lab} = 4.88$ GeV the number of dilepton pairs is likely to be overestimated experimentally in the mass range $M = 300 \div 700$ MeV.

PACS numbers: 25.75.Dw, 13.30.Ce, 12.40.Yx

§ E-mail address: christian.fuchs@uni-tuebingen.de

1. Introduction

Relativistic heavy-ion collisions present an unique possibility to create nuclear matter at high densities and temperatures where the hadron properties become different and a phase transition to quark matter with signatures of the deconfinement and restoration of chiral symmetry is expected. The change of the nucleon mass in the nuclear matter was implemented into the Walecka model [1, 2] already in 1970's in the framework of the effective hadron field theory. Later on this effect was put on the firmer grounds on the basis of a partial restoration of the chiral symmetry and finite-density QCD sum rules [3, 4], the Nambu-Jona-Lasinio model [5], and effective meson field theory [2, 6, 7].

Dileptons (e^+e^- , $\mu^+\mu^-$) are the most clear probes of the high density nuclear matter. The reason is that the dileptons interact with the matter only by electromagnetic forces and can therefore leave the heavy-ion reaction zone essentially undistorted by final state interactions. They provide valuable information on the in-medium properties of hadrons and, hence, on the state of matter.

The dilepton spectra from heavy-ion collisions have been measured at two different energy scales: by the CERES and HELIOS-3 Collaborations at SPS [8, 9] (a few hundreds GeV per nucleon) and by the DLS Collaboration at BEVALAC [10] (a few GeV per nucleon). In the CERES and HELIOS-3 experiments and in the BEVALAC experiment the production of dileptons with invariant masses between $300 \div 700$ MeV is found to be enhanced as compared to estimates based on the theoretically known dilepton sources when in-medium modifications of hadron properties are neglected.

The data on the total photoabsorption cross section on heavy nuclei [11] give an evidence for the broadening of nucleon resonances in the nuclear medium [12]. The physics behind is the same as in the collision broadening of the atomic spectral lines in hot and dense gases, discussed by Weisskopf in the early 1930's [13] (for the present status of this field, see, e.g., [14]). This rather general effect which takes its origin from the atomic spectroscopy should also lead to a broadening of the ρ -mesons in heavy-ion collisions.

The low-energy dilepton excess can be explained by a reduction of the ρ -meson mass in a dense medium [15, 16, 17]. The in-medium modification of the ρ -meson spectral function [18, 19] leading to a broadening of the ρ -meson seems also to be sufficient to account for the CERES and HELIOS-3 data [17].

In the DLS experiment a different temperature and density regime is probed. The enhancement of the dilepton spectra due to the reduction of the ρ -meson mass and the ρ -meson broadening is not sufficient to bring theoretical estimates in coincidence with the available experimental data [20]. The in-medium ρ -meson scenarios that successfully explain the dilepton yield at SPS energies fail for the DLS data. This phenomenon was called the "DLS puzzle". It worthwhile to notice that the final data from the DLS Collaboration have changed by about a factor of 5 – 7 as compared to the initially reported results. The future HADES experiment at GSI will study the dilepton spectra at the same energy range in greater details [21].

A possibility to clarify the origin of the DLS puzzle has appeared since data from elementary pp (pd) collisions at $T = 1 \div 5$ GeV (T is the kinetic energy of the incident proton in the laboratory frame) became available from the DLS Collaboration [22]. The elementary cross sections enter as an input into the transport simulations of heavy-ion collisions, so their better understanding is of great value.

The dilepton spectra in the pp collisions at $T = 1 \div 5$ GeV have been calculated in

refs.[23, 24, 25]. In ref.[23] the agreement achieved with the DLS data is generally good at low energies where the subthreshold production of nucleon resonances is important. When the energy increases and the inclusive production becomes dominant, the dilepton yield is underestimated at the same mass range 300÷700 MeV as in the heavy-ion collisions. A signature for this effect exists also in the calculations of refs.[24, 25]. This can be interpreted to mean that the studies [23, 24, 25] revealed, apparently, the reoccurrence of the DLS puzzle on the elementary level of the nucleon collisions. They leave, therefore, a doubt on the quality of the experimental data and/or the reliability of the accepted theoretical schemes.

This paper is devoted to a further going theoretical analysis of the elementary dilepton production cross sections.

In the next Sect., the production mechanisms are critically revisited. The subthreshold production cross sections for the vector mesons are treated such that no double counting appears with the inclusive processes. The effect of multiple pion production on the experimental detection efficiency for the dilepton pairs is also studied. We demonstrate that the detector efficiency is sensitive to the number of pions produced and propose a simple model to account for the multiple pion production effects.

In the Dalitz decays of the nucleon resonances, $R \rightarrow Ne^+e^-$, the Vector Meson Dominance (VMD) model is usually applied for the description of the resonance transition form factors. However, the naive VMD which takes the $R \rightarrow N\rho$ data as an input systematically overestimates the radiative decay branchings. In Sect.3, the VMD model is extended to ensure the correct asymptotic behavior of the transition form factors in agreement with the quark counting rules. Such a modification is found to be sufficient to achieve an unified description of both, $R \rightarrow N\gamma$ radiative decays and $R \rightarrow N\rho(\omega)$ meson decays. Our estimates of the subthreshold cross sections rely therefore on the two essentially different sets of the experimental data, $R \rightarrow N\gamma$ and $R \rightarrow N\rho$. The numerical results are discussed in Sect.4. We found that the above improvements do not eliminate the discrepancy with the DLS data at $T = 4.88$ GeV. Moreover, the results for the lowest energy, $T = 1.04$ GeV, also require an additional study from the experimental and/or theoretical side.

2. $pp \rightarrow e^+e^-X$ reaction

The dilepton production in nucleon collisions goes through the production of virtual photons which decay subsequently into e^+e^- pairs. According to the VMD model, the virtual photons are coupled to vector mesons $V = \rho^0, \omega$, and ϕ . The dilepton production can therefore be calculated using the inclusive vector meson production cross sections:

$$\frac{d\sigma(s, M)^{pp \rightarrow e^+e^-X}}{dM^2} = \sum_V (1 + n_V) \frac{d\sigma(s, M)^{pp \rightarrow V X}}{dM^2} B(M)^{V \rightarrow e^+e^-}. \quad (1)$$

Here, s is the square of the invariant mass of two colliding protons, M the invariant mass of the dilepton pair, $d\sigma(s, M)^{pp \rightarrow V X}/dM^2$ is the differential vector meson production cross section, and n_V is the average number of additional vector mesons V in the state X . In the energy range of interest, $T = 1 \div 5$ GeV, where T is the kinetic energy of the proton in the laboratory system, $n_V = 0$. The branching ratio

$$B(M)^{V \rightarrow e^+e^-} = \frac{\Gamma(M)^{V \rightarrow e^+e^-}}{\Gamma_{tot}^V(M)} \quad (2)$$

corresponds to the direct $V \rightarrow e^+e^-$ decays, with $\Gamma_{tot}^V(M)$ being the total meson decay width.

In order to disentangle the various contributions, we decompose the cross section entering into eq.(1) into pole and background parts:

$$d\sigma(s, M)^{VX} = d\sigma(s, M)_P^{VX} + d\sigma(s, M)_B^{VX}. \quad (3)$$

Such a decomposition implies that interference effects between the different sources are neglected. The background sources like $\pi \rightarrow \gamma e^+e^-$ and $\eta \rightarrow \gamma e^+e^-$ do not interfere due to the kinematical reasons. These two reactions in turn do not interfere with the reaction $\omega \rightarrow \pi^0 e^+e^-$, since the final states are different. The reactions $NN \rightarrow RN$, $R \rightarrow e^+e^-X$ going through the nucleon resonances R with different quantum numbers do not interfere with each other either. The sources like $NN \rightarrow N\Delta(1232)$, $\Delta(1232) \rightarrow Ne^+e^-$ and $NN \rightarrow NN\rho$, $\rho \rightarrow e^+e^-$ do interfere, however. The relative phases of the amplitudes describing the different reactions are unknown, so the neglection of the interference between all the reactions constitutes a reasonable first approximation.

The distribution over the meson mass M in the pole part of the cross section has a Breit-Wigner form corrected to the available phase space for the final state VX . At moderate energies, the state X is dominated by two nucleons and pions, so one can write

$$\begin{aligned} d\sigma(s, M)_P^{VX} &= \sigma(s)_P^{VX} \frac{1}{\pi} \frac{M\Gamma_{tot}^V(M)dM^2}{(M^2 - m_V^2)^2 + (M\Gamma_{tot}^V(M))^2} \\ &\times \sum_{n=0}^N w_n C_n \Phi_{3+n}(\sqrt{s}...) \end{aligned} \quad (4)$$

where

$$\Phi_{3+n}(\sqrt{s}...) = \Phi(\sqrt{s}, m_N, m_N, M, \mu_\pi, \dots, \mu_\pi) \quad (5)$$

is the $(3+n)$ -body phase space of the final state (two nucleons with masses m_N , one vector meson V with mass m_V , and n pions with masses μ_π). The value $N_\pi = [(\sqrt{s} - 2m_N - m_V)/\mu_\pi]$ is the maximal number of pions allowed by energy conservation, $[x]$ denotes the integer value of x , and the values w_n are the probabilities for the production of n pions, with

$$\sum_{n=0}^{N_\pi} w_n = 1. \quad (6)$$

The normalization factor C_n is given by

$$C_n^{-1} = \int_{\mu_0^2}^{(\sqrt{s} - 2m_N - n\mu_\pi)^2} \frac{1}{\pi} \frac{M\Gamma_{tot}^V(M)dM^2}{(M^2 - m_V^2)^2 + (M\Gamma_{tot}^V(M))^2} \Phi_{3+n}(\sqrt{s}...) \quad (7)$$

where μ_0 is the physical threshold for vector meson decays ($\mu_0 = 2\mu_\pi$ for the ρ -meson). Notice that the cross section (3) vanishes at values $M < \mu_0$. However, the total width $\Gamma_{tot}^V(M)$ entering into the denominator of the branching ratio (2) at $M < \mu_0$ vanishes as well, so that the cross section (1) is actually finite everywhere above the two-electron threshold.

In the zero-width limit, $\Gamma_{tot}^V(M) = 0$, eq.(4) simplifies to give

$$d\sigma(s, M)_P^{VX} = \sigma(s)_P^{VX} \delta(M^2 - m_V^2) dM^2. \quad (8)$$

The finite-width effects are important for the ρ -meson and less important for ω - and ϕ -mesons.

As the background we consider states with π -mesons originating from the V -meson strong decays, that do not contribute to the pole part of the cross section of V -meson production. We assume *e.g.* that the ρ -mesons from the reactions

$$\begin{aligned}\pi^0 &\rightarrow \gamma\rho^0 \rightarrow \gamma e^+ e^- (\gamma\pi^+\pi^-), \\ \eta &\rightarrow \gamma\rho^0 \rightarrow \gamma e^+ e^- (\gamma\pi^+\pi^-), \\ \omega &\rightarrow \pi^0\rho^0 \rightarrow \pi^0 e^+ e^- (\pi^0\pi^+\pi^-), \\ R &\rightarrow N\rho^0 \rightarrow Ne^+ e^- (N\pi^+\pi^-)\end{aligned}$$

form a background, which should be added to the pole part of ρ -mesons production. (In the last line only the ρ -mesons away from the resonance region correspond to background.)

The dilepton invariant mass in all these reactions can be lower than the two-pion threshold. Clearly, all processes with $M < 2\mu_\pi$ are not accounted for by the pole part of the inclusive cross section. Their contributions should be added to the contribution of the pole part. With increasing invariant dilepton mass, somewhere in the region $M \approx m_\rho$, we come to the double counting problem. This part of the spectrum from the above reactions must be excluded as outlined below.

Experimental data on the exclusive cross sections $\sigma(s)_P^{VX}$ with $X = n\pi NN$ at $n \geq 1$ are not available. Here we assume that the probabilities w_n are described by a binomial distribution

$$w_n = \frac{N_\pi!}{n!(N_\pi - n)!} p^n (1-p)^{N_\pi - n}. \quad (9)$$

To fix all probabilities it is sufficient to know the ratio between the exclusive vector meson production cross section $\sigma(s)_P^{VNN}$ and the inclusive cross section $\sigma(s)_P^{VX}$. These two cross sections are experimentally known [27]. The value N_π is defined as above by energy conservation while the value p can be extracted from the relation

$$\frac{\sigma(s)_P^{VNN}}{\sigma(s)_P^{VX}} = (1-p)^{N_\pi}. \quad (10)$$

The pion multiplicity equals

$$n_\pi = \sum_{n=0}^{N_\pi} n w_n = p N_\pi. \quad (11)$$

In the case of the ρ -meson, the cross section $\sigma(s)_P^{VX}$ determines the pole behavior of the total cross section $d\sigma(s, M)^{\pi^+\pi^-X}$ in the vicinity of the ρ -meson peak. Like for vector mesons, eq.(3), the total cross section $d\sigma(s, M)^{\pi^+\pi^-X}$ for the 2π production can be decomposed into ρ -pole and background parts

$$d\sigma(s, M)^{\pi^+\pi^-X} = d\sigma(s, M)_P^{\rho^0 X} + d\sigma(s, M)_B^{\pi^+\pi^-X}. \quad (12)$$

The background parts on the right hand sides of eq.(12) and eq.(3) do not coincide since the $\pi^+\pi^-$ quantum numbers are not necessarily equal to the quantum numbers of the ρ -meson (this is the case at the ρ -meson peak only and this is why with $V = \rho^0$ the first terms in eq.(3) and eq.(12) coincide). Thus the left hand sides of eq.(12) and eq.(3) do not coincide as well. Since the ρ -meson is always detected via 2π final states

(or via 3π and $2K$ final states for ω - and ϕ -mesons, respectively), the inclusive cross section for the production of vector mesons which enters into eq.(1) cannot be uniquely determined from the experimental data on inclusive production of $\pi^+\pi^-$. Instead, one needs a model for the calculation of the background part of the cross section in eq.(3). A subtle problem of double counting in the total dilepton production cross section appears in this way. We propose a quite natural phenomenological solution for it.

The background term $d\sigma(s, M)\rho_B^{0X}$ at $X \neq NN$ can be saturated, at least partially, by considering the production of light mesons: $pp \rightarrow \eta X \rightarrow \rho^0 \gamma X \rightarrow \pi^+ \pi^- \gamma X$, $pp \rightarrow \omega X \rightarrow \rho^0 \pi^0 X \rightarrow \pi^+ \pi^- \pi^0 X$, etc., similarly for the ω - and ϕ -mesons. The $\pi^+ \pi^-$ invariant masses are small here, so these processes contribute to the $\pi^+ \pi^-$ background. Eq.(1) can now be rewritten as follows

$$d\sigma(s, M)^{e^+ e^- X} = d\sigma(s, M)_P^{e^+ e^- X} + d\sigma(s, M)_B^{e^+ e^- X} \Big|_{X=NN} + d\sigma(s, M)_B^{e^+ e^- X} \Big|_{X \neq NN}. \quad (13)$$

The first term is the same as in Eq.(1), i.e. with the sum running over all vector mesons, however, keeping only the pole part of the cross section. In Eq.(13) the background is divided into contributions from direct decays of intermediate vector mesons, which are off-shell and typically below their physical thresholds ($X = NN$) and from decays of intermediate mesons, \mathcal{M} , to multi-particle final states ($X \neq NN$). In the latter case, the cross section for the production of the intermediate meson has to be folded over its branching ratio to the final state under consideration:

$$\frac{d\sigma(s, M)_B^{e^+ e^- X}}{dM^2} \Big|_{X \neq NN} = \sum_{\mathcal{M}} \int d\mu^2 (1 + n_{\mathcal{M}}) \times \frac{d\sigma(s, \mu)^{\mathcal{M}X'}}{d\mu^2} \frac{dB(\mu, M)^{\mathcal{M} \rightarrow e^+ e^- X''}}{dM^2}. \quad (14)$$

The sum runs over the mesons $\mathcal{M} = \pi$, η , ρ , ω , and ϕ . Here, $n_{\mathcal{M}}$ is the average number of mesons \mathcal{M} in the state X' . The value μ in the last equation describes the distribution over the off-shell masses of the mesons. For pseudo-scalar mesons, the cross sections due to their small widths are proportional to the delta-function $\delta(\mu^2 - m_{\mathcal{M}}^2)$ (cf. Eq.(8)) and the expression reduces to a sum over the on-shell mesons decaying to the states $e^+ e^- X''$ with $X'' \neq \emptyset$, $X = X' + X''$. For vector mesons entering the sum of Eq.(14) one should use the cross sections (3) whose pole components are well defined.

The contribution to the background part of the cross section (1) with $X = NN$ can be calculated assuming that it results from subthreshold decays of baryon resonances $R = \Delta(1232)$, $N(1520)$, ... produced in pp collisions, which decay into nucleons and vector mesons, $R \rightarrow NV$ [25]. In terms of the branching ratios for the Dalitz decays of the baryon resonances, the cross section can be written as follows

$$\frac{d\sigma(s, M)_B^{e^+ e^- X}}{dM^2} \Big|_{X=NN} = \sum_R \int_{(m_N + M)^2}^{(\sqrt{s} - m_N)^2} d\mu^2 \frac{d\sigma(s, \mu)^{pp \rightarrow pR}}{d\mu^2} \times \sum_V \frac{dB(\mu, M)^{R \rightarrow V p \rightarrow e^+ e^- p}}{dM^2}. \quad (15)$$

Here, μ is the running mass of the baryon resonance R with the cross section $d\sigma(s, \mu)^{pp \rightarrow pR}$, $dB(\mu, M)^{R \rightarrow Vp \rightarrow e^+ e^- p}$ is the differential branching ratio for the Dalitz decay $R \rightarrow e^+ e^- p$ through the vector meson V .

With increasing energy, the vector mesons in Eq.(15) can be produced at their physical masses. In such a case, the processes (15) contribute to the pole part of the cross section $d\sigma(s, M)^{e^+ e^- X}$. The pole part of inclusive cross sections by definition accounts for all possible sources for the appearance of on-shell vector mesons, so that a naive extension of the subthreshold cross section to higher energies would result in a double counting. To avoid this double counting we should skip the exclusive part of vector meson production in pp collision that enters to the total inclusive production of vector mesons as already taken into account in Eq.(15):

$$d\sigma(s) = d\sigma(s)^{incl}(1 - w_0) + d\sigma(s)^{subth} \quad (16)$$

The factor $1 - w_0$ excludes the $NNe^+ e^-$ component of the inclusive cross section which is reproduced by the subthreshold mechanizm. This prescription lies on the comparison of the experimental data to the exclusive vector meson production cross section, that goes through baryon resonances

$$\begin{aligned} \sigma(s)^{VX} |_{X=NN} &= \sum_R \int_{(m_N+M)^2}^{(\sqrt{s}-m_N)^2} d\mu^2 \frac{d\sigma(s, \mu)^{pp \rightarrow pR}}{d\mu^2} \\ &\times \int \frac{dB(\mu, M)^{R \rightarrow Vp}}{dM^2} dM^2. \end{aligned} \quad (17)$$

The cross sections reasonably agree (see Figs. 1 and 2).

The meson multiplicities $n_{\mathcal{M}}$ in Eq.(14) are set equal to zero except for the neutral pions. For pions, we assume $n_{\pi^0} = \frac{1}{2}n_{\pi}$ where n_{π} is given by Eq.(11). The factor $\frac{1}{2}$ appears statistically in the limit $n \rightarrow \infty$ from charge conservation which implies that in every channel the total number of the neutral-pion pairs $\pi^0\pi^0$ must be equal to the number of the charged-pion $\pi^+\pi^-$ pairs.

There are no experimental data on the pion production inclusive cross section $\sigma(s, \mu_{\pi})^{pp \rightarrow \pi^0 X}$ at $T = 1 \div 5$ GeV. There exist, however, experimental data on the two-pion production cross sections $\sigma(s, \mu_{\pi})^{pp \rightarrow \pi\pi NN}$ [28]. The parameter p of the pion number distribution can therefore be estimated from equation

$$\frac{\sigma(s)^{\pi^0\pi NN}}{\sigma(s)^{\pi^0 pp}} = \frac{pN_{\pi}}{1-p}. \quad (18)$$

It can further be used to find the total inclusive cross section $\sigma(s, \mu_{\pi})^{pp \rightarrow \pi^0 X}$ using the same relation as in Eq.(10). The results for the pion multiplicities produced in reactions in accordance with different mesons \mathcal{M} are summarized in Table 1 for those values of kinetic energies, T , at which the dilepton cross sections are measured by the DLS collaboration. We give there also the cross sections obtained from the interpolation and/or extrapolation between the available experimental points. The accuracy of these estimates is rarely better than 20%. For the pion, we give an estimate for the inclusive cross section. Notice that it is in reasonable agreement with the prediction from the UrQMD transport model [23].

For mesons $\mathcal{M} = \eta, \rho, \omega$, and ϕ , estimates for the cross sections $pp \rightarrow \mathcal{M}\pi NN$ are given as derived from the distribution (9).

Also the estimates for the exclusive multi-pion production cross are in line with prediction from the FRITIOF string fragmentation model [29] and the calculation of ref.[30]. To show this we make the following comparisons:

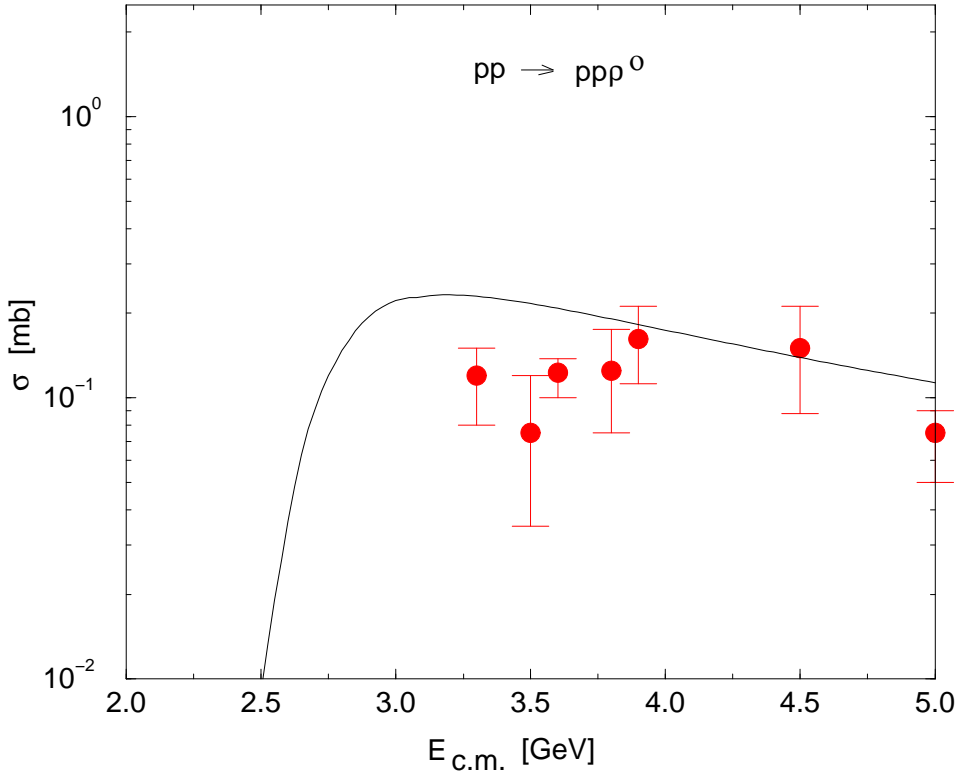


Figure 1. Exclusive ρ^0 meson production in proton-proton collision calculated over contribution of intermediate baryon resonances (17) compared to experimental data.

First, we compare our simple formulas explicitly to FRITIOF. In refs.[31, 32] an attempt was made to extrapolate the FRITIOF model, originally proposed for high energies, to lower energies by a modification of the two-body mechanism for inelastic hadron-hadron reactions. The authors claimed that they got finally a reasonable description of the basic characteristics of the hadron-hadron and nucleus-nucleus collisions, within the modified FRITIOF model.

We compare our model with the modified FRITIOF model of refs.[31, 32] for the reaction $np \rightarrow pp\pi^-X$ at $P_{lab} = 3.83$ GeV and 5.1 GeV. In Table 2, we show 4 channels with $X = \emptyset, \pi^0, \pi^+\pi^-, \pi^+\pi^-\pi^0$. The cross sections for the channels $X = \pi^0\pi^0, \pi^0\pi^0\pi^0$ are not available. We assume

$$\sigma(np \rightarrow pp\pi^-\pi^0\pi^0) = \sigma(np \rightarrow pp\pi^-\pi^+\pi^-), \quad (19)$$

$$\sigma(np \rightarrow pp\pi^-\pi^0\pi^0\pi^0) = \sigma(np \rightarrow pp\pi^-\pi^+\pi^-\pi^0). \quad (20)$$

We use the experimental data from the first and the last lines of the Table 2 to fit the parameter p of the binomial distribution. The results are shown in the Table 2 (third lines in the boxes), together with the experimental data (first lines of the boxes, numbers with errors) and predictions of the modified FRITIOF model (second lines

Table 1. The maximum number of pions, N_π , the average pion multiplicities, n_π , and the cross sections $\sigma^{\mathcal{M}\pi NN}$, $\sigma^{\mathcal{M}NN}$, and $\sigma^{\mathcal{M}X}$ for production of mesons $\mathcal{M} = \pi^0$, η , ρ , ω , and ϕ in the proton-proton collisions for the set of energies $T = 1.04$, 1.27 , 1.61 , 2.09 , and 4.88 GeV, at which the dilepton production cross section has been measured by the DLS Collaboration. The last three lines with the cross sections contain $3 \times 12 = 36$ numbers. The 24 numbers are compilation of the available experimental data, while the 12 numbers marked with the symbol “#” are predictions from our binomial formula (9). The experimental cross sections are measured at energies different from the BEVALAC energies, so we give interpolations from the available experimental points.

T [GeV]	1.04	1.27	1.61	1.85	1.85	2.09
\mathcal{M}	π^0	π^0	π^0	π^0	η	π^0
N_π	2	3	3	4	1	5
n_π	0.09	0.20	0.56	0.74	0.26	1.07
$\sigma^{\mathcal{M}\pi NN}$ [mb]	0.4	0.9	2.7	3.4	4.9	0.05#)
$\sigma^{\mathcal{M}NN}$ [mb]	4.5	4.2	3.9	3.8	0.13	3.6
$\sigma^{\mathcal{M}X}$ [mb]	4.9#)	5.2#)	7.3#)	8.5#)	0.17	12#)
T [GeV]	2.09	4.88	4.88	4.88	4.88	4.88
\mathcal{M}	η	π^0	η	ρ^0	ω	ϕ
N_π	2	11	8	6	6	4
n_π	0.55	1.80	1.87	1.67	1.36	1.54
$\sigma^{\mathcal{M}\pi NN}$ [mb]	0.11#)	5.8	0.34#)	0.28#)	0.35#)	0.003#)
$\sigma^{\mathcal{M}NN}$ [mb]	0.14	2.7	0.14	0.12	0.20	0.001
$\sigma^{\mathcal{M}X}$ [mb]	0.27	19#)	1.19	0.94	0.94	0.007

Table 2. The multipion production cross sections estimated in the FRITIOF model (second line) and from the binomial distribution (third line) for the proton beam momentum of $P_{lab} = 3.83$ and 5.1 GeV. Given in the first line are the experimental data.

P_{lab} [GeV]	3.83	5.1
$np \rightarrow pp\pi^-$	2.35 ± 0.12 (1.62) 2.35	2.13 ± 0.11 (1.75) 2.13
$np \rightarrow pp\pi^-\pi^0$	1.83 ± 0.13 (3.03) 2.05	2.05 ± 0.12 (2.60) 2.99
$np \rightarrow pp\pi^-\pi^+\pi^-$	0.31 ± 0.04 (0.41) 0.38	0.56 ± 0.04 (0.90) 0.93
$np \rightarrow pp\pi^-\pi^0\pi^+\pi^-$	0.08 ± 0.01 (0.06) 0.08	0.34 ± 0.03 (0.28) 0.34

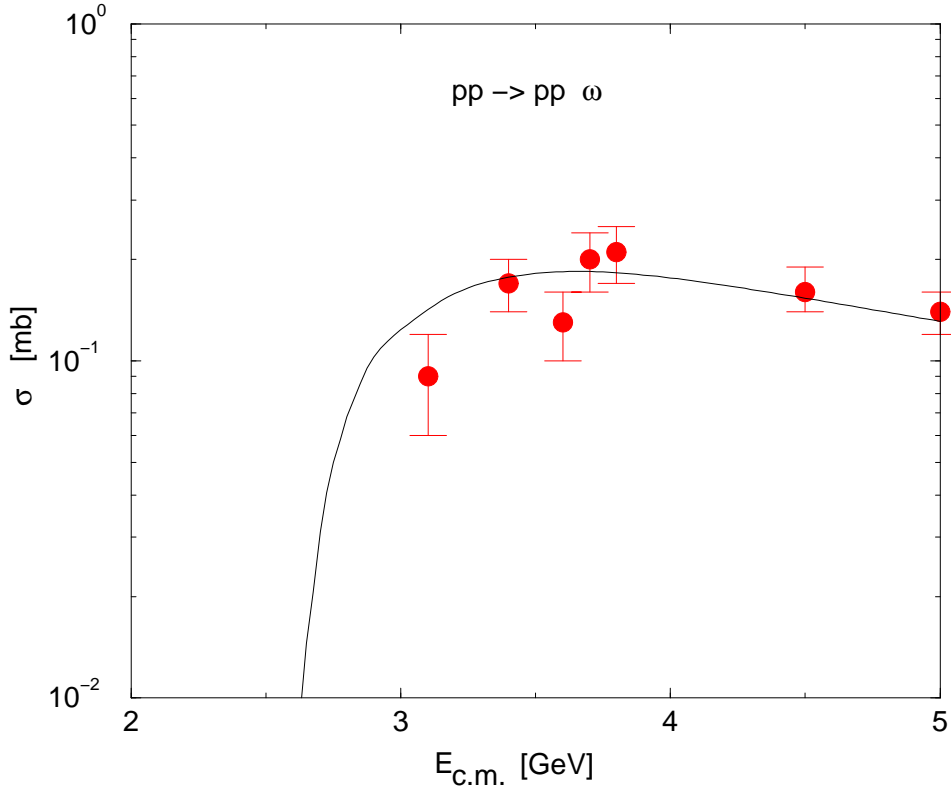


Figure 2. Exclusive ω meson production in proton-proton collision calculated over contribution of intermediate baryon resonances (17) compared to experimental data.

of the boxes, numbers in the brackets). The experimental data are from ref. [33]. It is seen that the description is reasonable. Notice that a 30% accuracy occur for the modified FRITIOF predictions and similarly 30% is also the accuracy of the binomial formula predictions.

Second, the agreement with the work [30] is reasonable. For example as it can be seen from Table 2 that our value for $\sigma(np \rightarrow pp\pi^-\pi^0)$ at 5.1 GeV is close to their result of 2.85 mb at 5.5 GeV.

In Table 3, we compare predictions from the binomial distribution for the reaction $pp \rightarrow pp\pi^0X$ with the experimental data from ref.[26]. The uncertainty exists in these data also: the cross sections for $X = \pi^0, \pi^0\pi^0, \pi^0\pi^0\pi^0, \pi^0\pi^+\pi^-, \pi^0\pi^0\pi^0\pi^0$, and $\pi^0\pi^0\pi^-\pi^+$ are unknown. For a qualitative estimate, we assume like before that the cross sections for the unknown channels are equal to the cross sections for the known channels, with the same number of the pions. The parameter p of the binomial formula is determined at each energy from the channels with one pion and with the maximum number of the pions in the final states.

The agreement is not unreasonable, especially in the view of the naive approximations like (19) and (20). The binomial formula does not contradict to the

Table 3. The multipion production cross sections in proton-proton collisions estimated from the binomial distribution for different momenta of the beam proton (first column). The second column shows the final states, the third one shows the parameter p of the binomial distribution, the next column gives the estimated cross sections in mb , and the last one gives the experimental numbers in mb .

$P_{lab} [GeV]$	final state	p	$\sigma^{binom} [mb]$	$\sigma^{expt} [mb]$
5.5	$pp\pi^0$	0.127	2.77	2.77 ± 0.11
5.5	$pp\pi^+\pi^-$	0.127	4.04	2.84 ± 0.08
5.5	$pp\pi^+\pi^-\pi^0$	0.127	1.327	1.81 ± 0.07
5.5	$pp\pi^+\pi^-\pi^+\pi^-$	0.127	0.516	0.227 ± 0.023
5.5	$pp\pi^+\pi^-\pi^+\pi^0$	0.127	0.088	0.088 ± 0.014
3.68	$pp\pi^0$	0.134	2.950	2.95 ± 0.31
3.68	$pp\pi^+\pi^-$	0.134	3.213	2.72 ± 0.13
3.68	$pp\pi^+\pi^-\pi^0$	0.134	0.750	0.75 ± 0.07
2.81	$pp\pi^0$	0.095	3.600	3.60 ± 0.21
2.81	$pp\pi^+\pi^-$	0.095	1.897	2.35 ± 0.14
2.81	$pp\pi^+\pi^-\pi^0$	0.095	0.200	0.20 ± 0.03
2.23	$pp\pi^0$	0.054	4.060	4.06 ± 0.27
2.23	$pp\pi^+\pi^-$	0.054	0.697	1.24 ± 0.14
2.23	$pp\pi^+\pi^-\pi^0$	0.054	0.020	0.02 ± 0.02

available data and we suppose that it can be used for estimates of the multiple pion production effects. Notice that the pion contribution to the dilepton spectrum is quite far from the really interesting region about and just below the ρ -meson peak.

For the mesonic dilepton decays of mesons $\mathcal{M} \rightarrow e^+e^-X$, experimental data exist in most cases. The radiative decays $\mathcal{M} \rightarrow \gamma X$ can further be used to calculate the dilepton decays when the experimental data are not available. For details of the determination of the various branching ratios see ref.[34]. The inclusive cross sections for the meson production and the branching ratios for the mesonic decays to dileptons can be combined to estimate the dilepton yield from Eq.(13).

The differential decay branchings $dB^{R \rightarrow Ne^+e^-}(\mu, M)/dM^2$ are calculated in ref.[25] in a non-relativistic approximation for the multipole decays with the emission of a massive vector particle. We follow a similar approach here, but consider the relativistic case and modify the transition form factors for the nucleon resonances, R , which is needed to bring their asymptotic behavior in the correspondence with the quark counting rules and to provide an unified description of the photo- and electroproduction data and vector meson decays $R \rightarrow N\rho(\omega)$ [38].

3. Transition form factors, quark counting rules, and radiative and vector meson decays of nucleon resonances

The problem is adequately formulated in the non-relativistic approximation for radiative and vector meson decays of nucleon resonances. We start with the discussion of this case, since it is much simpler. The relativistic treatment, which will finally be implemented into the consideration, although is more complicated, is motivated by the same physical ideas.

Table 4. The coupling constants $f_{RN\rho}$ derived from the $R \rightarrow N\rho$ mesonic decays are compared to the coupling constants $f_{RN\rho}^\gamma$ fixed from the radiative $R \rightarrow N\gamma$ decays. The numerical values $f_{RN\rho}$ are taken from ref. [19], with exception of the $\Delta(1232)$ resonance for which the theoretical value from [18] is given and of the $N(1440)$ and $N(1535)$ resonances where the results of our calculations are given.

R	N_{1440}	N_{1520}	N_{1535}	N_{1650}	N_{1680}	N_{1720}	Δ_{1232}	Δ_{1620}	Δ_{1700}	Δ_{1905}
J^P	$\frac{1}{2}^+$	$\frac{3}{2}^-$	$\frac{1}{2}^-$	$\frac{1}{2}^-$	$\frac{5}{2}^+$	$\frac{3}{2}^+$	$\frac{3}{2}^+$	$\frac{1}{2}^-$	$\frac{3}{2}^-$	$\frac{5}{2}^+$
$f_{RN\rho}$	< 26	7.0	< 2.0	0.9	6.3	7.8	15.3	2.5	5.0	12.2
$f_{RN\rho}^\gamma$	1.3	3.8	1.8	< 0.8	3.9	2.2	10.8	0.7	2.7	2.1

3.1. Vector meson decays of nucleon resonances in the nonrelativistic approximation

The description of the resonance decays $R \rightarrow N\gamma^*$, $\gamma^* \rightarrow e^+e^-$ is usually based on the VMD model which provides transition form factors $RN\gamma$ of a monopole form. The pole corresponds to the masses of the ρ - and ω -mesons. This model should give, in principle, an unified description of the radiative $RN\gamma$ and the mesonic RNV decays. However, a normalization to the radiative branchings ($RN\gamma$) strongly underestimates the mesonic branchings (RNV) as we discuss below.

The resonance $N(1520)$ is a case for which both, the $N(1520) \rightarrow N\rho$ and $N(1520) \rightarrow N\gamma$ widths are known with a relatively high precision: $B(N(1520) \rightarrow N\rho) = 15 \div 25\%$, $B(N(1520) \rightarrow N\gamma) = 0.46 \div 0.56\%$ ($p\gamma$ mode), $0.30 \div 0.53\%$ ($n\gamma$ mode). The branching ratios of the proton and neutron modes are equal within the experimental errors. Let us, for the moment, interpret this by assumption that the radiative mode is dominated by the ρ -meson. The same conclusion is reasonable for other N^* resonances: $B(N(1440) \rightarrow N\gamma) = 0.035 \div 0.048\%$ ($p\gamma$ mode), $0.009 \div 0.032\%$ ($n\gamma$ mode); $B(N(1535) \rightarrow N\gamma) = 0.15 \div 0.35\%$ ($p\gamma$ mode), $0.004 \div 0.29\%$ ($n\gamma$ mode), etc. The Δ decays proceed exclusively through the ρ -meson.

However, now the standard VMD model as it has been used in [25] leads to a severe inconsistency: Using the coupling constant $f_{N(1520)N\rho} = 7.0$ extracted from the mesonic $N(1520) \rightarrow N\rho$ decay, the branching ratio for the radiative decay is found to be two to three times greater than the experimental value. Analogous overestimations are observed almost for all other N and Δ resonances for which the experimental $N\rho$ and $N\gamma$ data are available. Table 4 summarizes the results.

The standard VMD predicts a $1/t$ asymptotic behavior for the transition form factors. However, quark counting rules require a stronger suppression at high t . It is known from the nucleon form factors, the pion form factor, and the $\omega\pi\gamma$ and $\rho\pi\gamma$ transition form factors that the quark counting rules start to work experimentally at moderate $t \sim 1$ GeV 2 . One can assume that an appropriate modification of the standard VMD which takes the correct asymptotics of the $RN\gamma$ transition form factors into account can provide a more accurate description of the radiative decays of the nucleon resonances.

We propose the following solution of the inconsistency between the RNV and $RN\gamma$ decay rates: Let radial excitations of the ρ -meson, the $\rho(1450)$ -meson and $\rho(1700)$ -meson, for example, interfere with the ρ -meson in radiative processes. However, we know neither the couplings of the $\rho(1450)$ and $\rho(1700)$ to the resonances ($f_{RN\rho'}$, $f_{RN\rho''}$) nor the couplings of the $\rho(1450)$ and $\rho(1700)$ to a photon ($g_{\rho'}$, $g_{\rho''}$).

Thus in the sum

$$\begin{aligned}\mathcal{M}(M^2) = \sum_{i=1}^3 \mathcal{M}_i &= \frac{f_{RN\rho}}{m_\rho} \frac{m_\rho^2}{g_\rho} \frac{1}{\tilde{m}_\rho^2 - M^2} + \frac{f_{RN\rho'}}{m_{\rho'}} \frac{m_{\rho'}^2}{g_{\rho'}} \frac{1}{\tilde{m}_{\rho'}^2 - M^2} \\ &+ \frac{f_{RN\rho''}}{m_{\rho''}} \frac{m_{\rho''}^2}{g_{\rho''}} \frac{1}{\tilde{m}_{\rho''}^2 - M^2},\end{aligned}$$

where $\tilde{m}_k^2 = m_k^2 - iM\Gamma_k$ with $k = \rho, \rho', \rho''$, and ρ'', ρ', ρ'' refer to $\rho(1450)$ - and $\rho(1700)$ -mesons, respectively, the coefficients $\frac{f_{RN\rho'}}{m_{\rho'}} \frac{m_{\rho'}^2}{g_{\rho'}}$ and $\frac{f_{RN\rho''}}{m_{\rho''}} \frac{m_{\rho''}^2}{g_{\rho''}}$ are unknown. According to the quark counting rules [40, 41], for large and negative M^2 the form factors of the $RN\gamma^*$ amplitudes decrease like $1/M^6$. On the phenomenological level we can attribute such a behavior to a cancellation between the ρ -, ρ' -, and ρ'' -mesons. The constants $\frac{f_{RN\rho'}}{m_{\rho'}} \frac{m_{\rho'}^2}{g_{\rho'}}$ and $\frac{f_{RN\rho''}}{m_{\rho''}} \frac{m_{\rho''}^2}{g_{\rho''}}$ are then fixed and we obtain

$$\mathcal{M}(M^2) = \frac{f_{RN\rho}}{m_\rho} \frac{m_\rho^2}{g_\rho} \frac{1}{\tilde{m}_\rho^2 - M^2} \left(\frac{\tilde{m}_{\rho'}^2 - \tilde{m}_\rho^2}{\tilde{m}_{\rho'}^2 - M^2} \right) \left(\frac{\tilde{m}_{\rho''}^2 - \tilde{m}_\rho^2}{\tilde{m}_{\rho''}^2 - M^2} \right). \quad (21)$$

The last two factors in Eq.(21) give the desired modification of the ρ -meson contribution to the radiative decays of the baryon resonances, as compared to the naive VMD model:

$$d\Gamma^{(R \rightarrow Ne^+e^-)}(\mu, M) = d\Gamma^{(R \rightarrow Ne^+e^-)}(\mu, M)^{(naive VMD)} F_\rho(M^2). \quad (22)$$

The mass-dependent correction factor is given by

$$F_\rho(M^2) = \left| \left(\frac{\tilde{m}_{\rho'}^2 - \tilde{m}_\rho^2}{\tilde{m}_{\rho'}^2 - M^2} \right) \left(\frac{\tilde{m}_{\rho''}^2 - \tilde{m}_\rho^2}{\tilde{m}_{\rho''}^2 - M^2} \right) \right|^2. \quad (23)$$

The same modification applies to the $R \rightarrow N\gamma$ decays. The reduction factor in the amplitude $R \rightarrow N\gamma$ equals $\sqrt{F_\rho(M^2=0)} = 0.56$. It is seen from Table 4 that a reduction of about $\frac{1}{2}$ is just what one needs for a consistent description of both, the ρ -meson and the radiative decay of the $N(1520)$. In all other cases the reduction factor also improves the agreement. In the case of the $\Delta(1905)$ resonance, the large difference between $f_{RN\rho}$ and $f_{RN\rho}^\gamma$ can be attributed to a further suppression of the amplitude $A(M^2)$ due to the quark counting rules which require a $1/M^8$ behavior of the $RN\gamma^*$ vertex for the $\frac{5}{2}^+ \rightarrow \frac{1}{2}^+$ transition. So, we have formulated the problem and outlined its possible solution.

Note that interference between the different ρ -meson states does not change essentially the dilepton contribution from the pion annihilation channel in heavy-ion collisions, since the ρ -meson form factor involved into that process falls off asymptotically like $1/t$ due to the quark counting rules, and so there should be no destructive interference between members of the ρ -meson family. The VMD model by Kroll, Lee and Zumino [35] allows two independent couplings for the photons and vector mesons and can be used to resolve the discrepancy between the photon and ρ -meson branchings of the nucleon resonances [36]. It provides, however, the form factors asymptotics $F(t) = O(1)$ in disagreement with the quark counting rules.

3.2. Relativistic treatment of the vector meson decays of nucleon resonances

The relativistic treatment of the $R \rightarrow NV$ decays is in details discussed in [37]. Here, we sketch out the basic concept. For nucleon resonances with spin $J > 1/2$

and arbitrary parity, there exist three independent transition form factors, while for spin-1/2 resonances, two independent form factors should be considered [42, 43, 44].

In terms of the electric (E), magnetic (M), and Coulomb (C) form factors, the decay widths of nucleon resonances with spin $J = l + 1/2$ into a virtual photon with mass M has the form [37, 38]:

$$\Gamma(N_{(\pm)}^* \rightarrow N\gamma^*) = \frac{9\alpha}{16} \frac{(l!)^2}{2^l (2l+1)!} \frac{m_\pm^2 (m_\mp^2 - M^2)^{l+1/2} (m_\pm^2 - M^2)^{l-1/2}}{m_*^{2l+1} m^2} \left(\frac{l+1}{l} \left| G_{M/E}^{(\pm)} \right|^2 + (l+1)(l+2) \left| G_{E/M}^{(\pm)} \right|^2 + \frac{M^2}{m_*^2} \left| G_C^{(\pm)} \right|^2 \right) \quad (24)$$

where m_* refers to the nucleon resonance mass, m is the nucleon mass, $m_\pm = m_* \pm m$. The signs \pm refer to the natural parity ($1/2^-, 3/2^+, 5/2^-, \dots$) and abnormal parity ($1/2^+, 3/2^-, 5/2^+, \dots$) resonances. $G_{M/E}^{\pm}$ means G_M^+ or G_E^- . The above equation is valid for $l > 0$. For $l = 0$ ($J = 1/2$), one gets

$$\Gamma(N_{(\pm)}^* \rightarrow N\gamma^*) = \frac{\alpha}{8m_*} (m_\pm^2 - M^2)^{3/2} (m_\mp^2 - M^2)^{1/2} \left(2 \left| G_{E/M}^{(\pm)} \right|^2 + \frac{M^2}{m_*^2} \left| G_C^{(\pm)} \right|^2 \right). \quad (25)$$

If the width $\Gamma(N^* \rightarrow N\gamma^*)$ is known, the factorization prescription can be used to find the dilepton decay rate:

$$d\Gamma(N^* \rightarrow Ne^+e^-) = \Gamma(N^* \rightarrow N\gamma^*) M \Gamma(\gamma^* \rightarrow e^+e^-) \frac{dM^2}{\pi M^4}, \quad (26)$$

where

$$M \Gamma(\gamma^* \rightarrow e^+e^-) = \frac{\alpha}{3} (M^2 + 2m_e^2) \sqrt{1 - \frac{4m_e^2}{M^2}} \quad (27)$$

is the decay width of a virtual photon γ^* into the dilepton pair with invariant mass M .

The couplings of the ρ - and ω - mesons and of their radial excitations can be taken into account to describe radiative and electroproduction helicity amplitudes satisfying the quark counting rules. The available data on the partial-wave analysis of the multichannel πN -scattering can also be included into the framework of the extended VMD model. In ref.[38], the parameters of the model are fixed by fitting those data and by taking into account quark model predictions when the experimental data are not available. In this work, we use the model [38] to calculate the dilepton production from the nucleon resonance decays.

In the relativistic case, we cannot write a compact expression for the suppression factor (23). However, it is clear that the effect does exist. The destructive interference is prescribed by the quark counting rules which are implemented into the relativistic model. It means that the radiative decay should be less probable as compared to the naive VMD estimate from the ground-state ρ -meson.

The medium can destroy the destructive interference, in which case one can expect an enhancement of the dilepton production below the ρ -meson peak [38]. A detailed treatment of this effect will be given elsewhere [39].

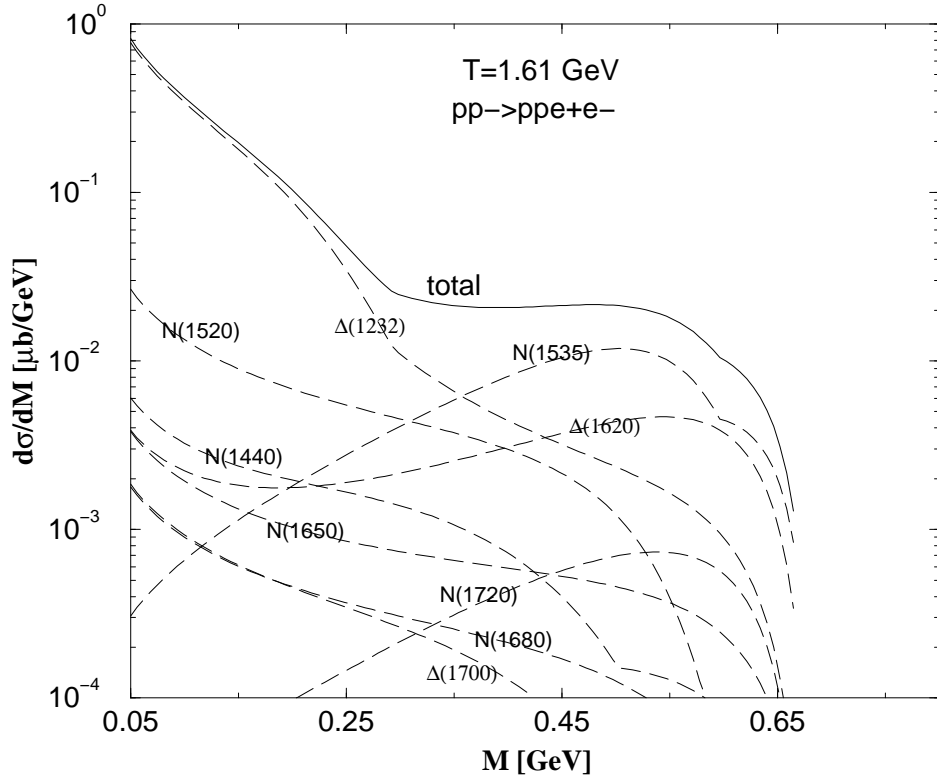


Figure 3. The dilepton production cross sections $pp \rightarrow e^+e^-pp$ through the nucleon resonances $R = \Delta$, N^* , and Δ^* at a kinetic proton energy of $T = 1.61$ GeV.

The $\Delta(1232)$ resonance is treated in the same way as the other resonances. We take into account 10 resonances listed in Table 4. The ρ - and ω -meson channels are treated on the same footing. The numerical results demonstrate that besides the $N(1520)$ and $\Delta(1232)$ resonances, the $N(1535)$ and $\Delta(1620)$ have considerable contributions. It can be seen from Fig. 3 where the resonance contributions are shown for proton kinetic energy $T = 1.61$ GeV. At moderate invariant masses $M \leq 0.35$ GeV of the dilepton pair, the resonance contributions are dominated by the $\Delta(1232)$. At larger masses $M \geq 0.35$ GeV, contributions from the heavier resonances become dominant.

4. Numerical results

The results for the dilepton spectra are shown in Fig. 4. We show also inclusive and subthreshold cross sections separately. To compare with the experimental data, the acceptance of the DLS detector with respect to the e^+e^- pairs that have invariant mass M , transverse momentum p_T , and rapidity y is taken into account. For each process, the distribution over the p_T and y is determined by the available phase space

of the process and then weighted with the filter function $f(M, p_T, y)$ provided by the DLS collaboration. The details of this procedure are described in Appendix B. Finally, the finite mass resolution of the detector, $\Delta M^{expt} = \pm 25$ MeV, is taken into account by smearing the spectra with a Gaussian distribution which corresponds to a standard error of $\sigma = 25$ MeV.

At the lowest initial kinetic energy of the proton, i.e. $T = 1.04$ GeV, the cross section is dominated by the π^0 -Dalitz decay below $M \leq 100$ MeV and by the Dalitz decays of the nucleon resonances, mainly the $\Delta(1232)$ -resonance, at $M \approx 200 \div 500$ MeV. Compared to our calculation there is an excess of detected e^+e^- pairs at $M \geq 300$ MeV. Earlier calculations [25] obtained higher cross sections in this mass range. This is due to the normalization to the $R \rightarrow N\rho$ branching ratios within the framework of the naive VMD which overestimates the radiative decay rates $R \rightarrow N\gamma$, as discussed in Sect.3.

At higher initial proton energies, the agreement with the DLS data is generally very reasonable. The contribution from the η -meson Dalitz decay is dominant at $M \approx 0.2 \div 0.4$ GeV, while the Dalitz decays of the baryon resonances dominate at $M \geq 400$ MeV.

For the proton kinetic energy $T = 2.09$ GeV, the inclusive and subthreshold productions of the ρ - and ω -mesons become important at $M \approx 800$ MeV. The ω -meson peak in the inclusive cross section is rather pronounced, whereas the subthreshold ω -meson production cross section is large and smooth. The total cross section, as a result, exceeds significantly the experimental data at $M \approx 0.7 \div 0.8$ GeV.

Refs.[23, 25] agree quite well with the experimental data at the ω -meson region. In ref.[23], the inclusive ω -peak is not reproduced, apparently, due to a stronger *ad hoc* smearing with a mass-dependent parameter $\sigma = 0.1M$. The smearing at the ω -meson peak turns out to be factor of 3 greater than it should ($\sigma = 80$ MeV instead of 25 MeV). In refs.[23, 25], the ω -channels from the nucleon resonance decays are neglected. This is the reason for the difference between our results and results of refs.[23, 25]. In our calculations, the ω -chanel contribution is large. It can only be lowered by price of an *ad hoc* reduction of the decay probabilities of the nucleon resonances into the vector mesons, which has been calculated using the quark models [45]. The quark models reproduce, however, the ρ -meson decays of the nucleon resonances quite well, i.e. they are in good agreement with the partial-wave analysis of the πN inelastic scattering [46]. In this way the experimental underestimation of the dilepton yield at the ω -peak at $T = 2.09$ GeV seems to contradict the πN inelastic scattering data.

Remarkably, the three highest experimental points at $T = 2.09$ GeV lie above the kinematical limit $M_{max} = \sqrt{s} - 2m_N \approx 850$ MeV and the indicated experimental error $\Delta M^{expt} = \pm 25$ MeV is not sufficient to explain their occurrence. We suppose that the experimental resolution is not good enough to resolve the kinematic threshold.

Finally, at $T = 4.88$ GeV, the contribution from the inclusive production of the η -, ρ -, and ω -mesons becomes dominant at $M \approx 300 \div 800$ MeV. There is an underestimation of the dilepton yield in the region $M \approx 400 \div 700$ MeV. A similar underestimation was found in [23] both, at $T = 2.09$ GeV and $T = 4.88$ GeV. As proposed in ref.[25], the existing gap might be filled by the subthreshold dilepton production via the baryon resonances. However, we were not able to match the data using a consistent description of the photoproduction data and the $R \rightarrow N\rho$ meson decay branchings, with the proper application of the Breit-Wigner formula (see details in Appendix 1), and removing possible sources for the double counting. Each of this three aspects leads to a reduction of the dilepton yield. Therefore, one

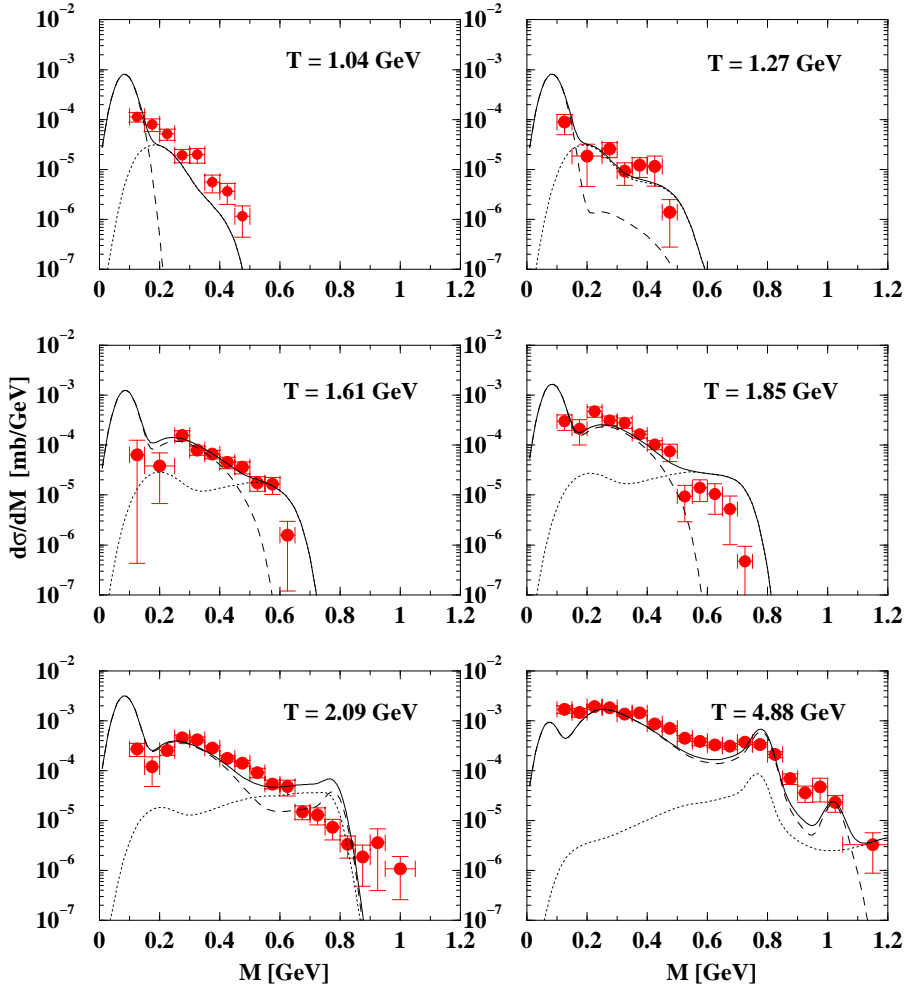


Figure 4. The differential dilepton production cross sections as a function of the dilepton invariant mass, M , after applying the experimental filter and the smearing procedure (see text). The solid curves are the total cross sections, the dashed curves correspond to the inclusive production, and the dotted curves correspond to the subthreshold production. The experimental data are from ref.[10].

cannot exclude that the origin of the so called "DLS puzzle" can be traced back to the elementary pp level and is not a specific feature of heavy-ion collisions. New experimental measurements of the dilepton cross section, especially at $T = 1.04, 2.09$, and 4.88 GeV, would certainly help to clarify this point.

In this context one should be aware that the comparison to the experimental data is strongly influenced by the acceptance of the DLS detector. In Appendix 2, we discuss the application of the corresponding filter program [22] for the calculation of the experimentally measured cross sections. In Fig.5 the effective detector efficiency, smeared by a Gaussian distribution with the standard deviation $\sigma = 25$ MeV, is shown as a function of the dilepton mass M for decays $\pi \rightarrow \gamma e^+ e^-$, $\eta \rightarrow \gamma e^+ e^-$, and

$\rho^0(\omega) \rightarrow e^+e^-$ at the two highest proton energies $T = 2.09$ GeV and $T = 4.88$ GeV, where the effects of the multiple pion production are most important. It can be seen that the effective acceptance decreases with increasing energy for a fixed number of pions in the final state. On the other hand, when the number of pions increases, the acceptance increases as well. This can be interpreted to mean that a larger number of the pions reduces the available phase space for mesons decaying to the dilepton pairs, and the decays of such mesons can be detected with better efficiency.

The effect is particularly strong for the $\pi \rightarrow \gamma e^+e^-$ decay at $T = 4.88$ GeV. While the average pion multiplicity n_π is around 2, the effective acceptance is extremely small below $n \approx 6$. The acceptance is not reliable when it is much smaller than unity. In our case this happens at $n \leq 6$. While the statistical distribution gives here, as we expect, reasonable estimates, the calculation of the part of the cross section connected to the additional production of $n \leq 6$ pions turns out to be unreliable. From the other side, at $n \geq 6$ the filter is well defined, but the binomial distribution gives exponentially small probabilities. The highest part of the pion spectra corresponding to $n \geq 6$ also cannot be calculated accurately. So, we consider the difference between our results for the pion contributions and those of refs.[23, 24] by about a factor of 3 and those of ref.[25] by about a factor of 6 as a conservative estimate for uncertainties inherent in the theoretical calculations for both, the distribution over the pion multiplicities and the experimental filter acceptance in the region of small invariant masses.

At lower energies, these uncertainties practically disappear. In Fig.5, we show a plot for the $\pi \rightarrow \gamma e^+e^-$ decay at $T = 2.09$ GeV. It can be seen that now already for $n = 0$ the effective acceptance is no more extremely small. For heavier mesons, the calculation of the acceptance is safer, which is again connected with less energy available for the produced mesons and, respectively, a better efficiency for the detection of the dileptons.

For the application of the filter we assumed an isotropic distribution of the particles in the final states in the c.m. frame. This is justified at small energies T . With increasing kinetic energy, the distribution acquires a bias towards the beam direction. This is an additional source of uncertainties in the calculations of the filter, which can be important at energy $T = 4.88$ GeV for the pion Dalitz decays.

The many-body phase spaces entering into Eq.(4) are known to be very sharp functions of the arguments. The Breit-Wigner distribution over the dilepton mass, M , gets therefore an enhancement towards small values of M . The greater the number of pions in the final state, the more important is this effect. We found that rare processes with probabilities $w_n \leq 0.03$ corresponding to large numbers of pions produced in association with the vector mesons, that should in principle give small contributions to the total cross sections, become very important at masses $M \leq 200 \div 300$ MeV. The spectral functions of the vector mesons are not known well far away from the vector meson peaks. This effect is thus beyond the scope of the present model. It should be analysed separately. In the present calculations, we apply a 3% criterion to the multiple pion processes: The values w_n are set equal to zero every time when $w_n < 0.03$. This works for the inclusive vector meson production at $T = 4.88$ GeV. At smaller energies pions are not produced in association with vector mesons.

5. Conclusion

We have considered the dilepton production in pp collisions at BEVALAC energies. The subthreshold production of vector mesons through the nucleon resonances is

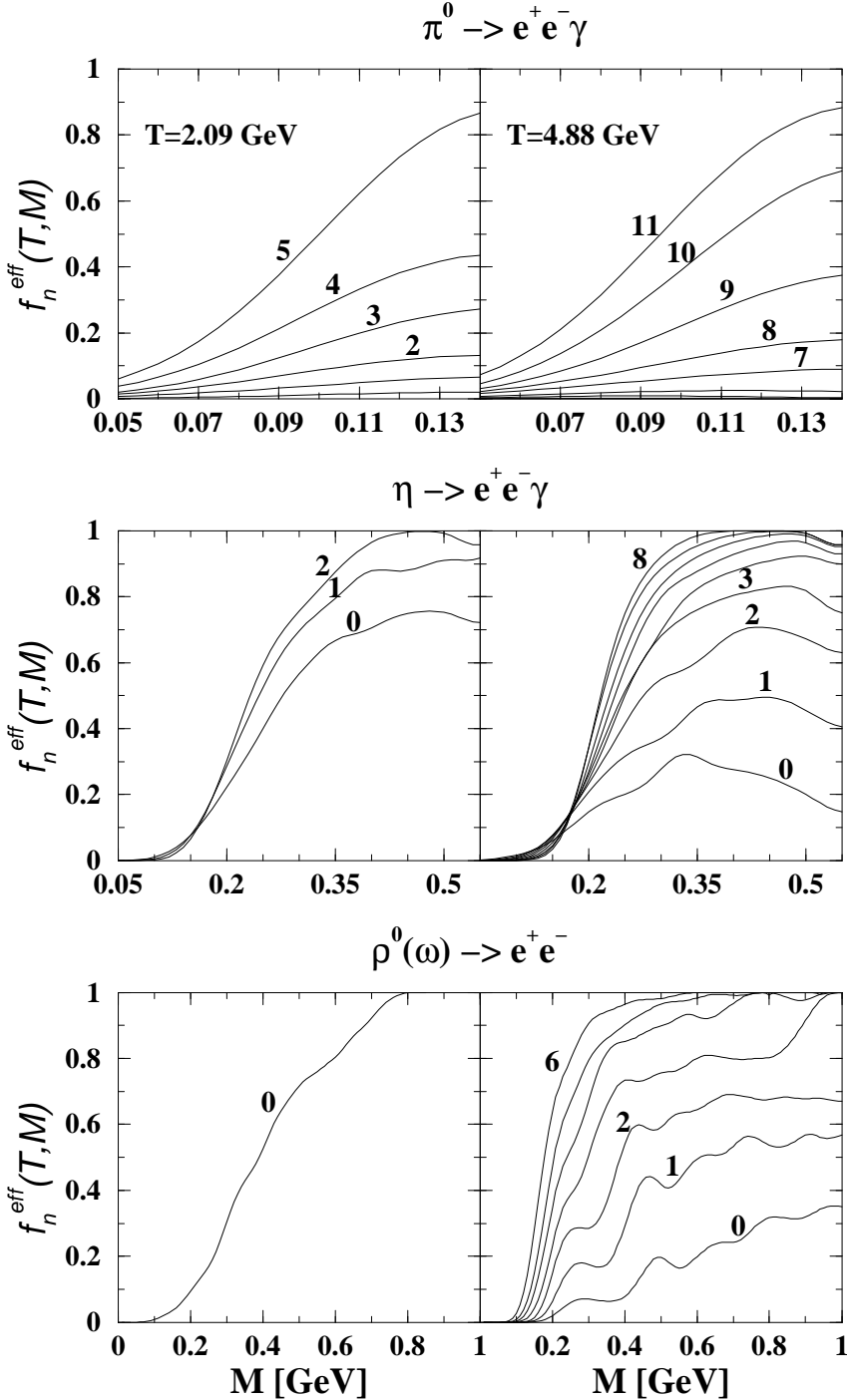


Figure 5. The effective acceptance of the DLS detector versus the invariant dilepton mass, M , for different numbers of pions, n , produced in association with the pion π^0 , η -meson, and $\rho^0(\omega)$ -mesons at two highest energies $T = 2.09$ and 4.88 GeV. The numbers over the curves show the numbers n of the pions.

described within the extended VMD model which allows to bring the transition form factors in agreement with the quark counting rules and provides an unified description of the photo- and electroproduction data, $\gamma(\gamma^*)N \rightarrow N^*$, the vector meson decays, $N^* \rightarrow N\rho(\omega)$, and the dilepton decays, $N^* \rightarrow N\ell^+\ell^-$. The dilepton decay rates are described relativistically using kinematically complete phenomenological expressions and numerical results of ref. [38]. In this context, we discussed also the problem of double counting and proposed its possible solution.

The resulting dilepton spectra are reasonably well described at proton energies ranging from $T = 1.27 \div 1.85$ GeV. At $T = 1.04$ GeV, there exists an overestimation of the dilepton yield, at $T = 2.09$ GeV, we see an underestimation in the vicinity of the ω -meson peak. At $T = 4.88$ GeV we observe an underestimation in the region of dilepton masses below the ρ -peak ($M \approx 400 \div 700$ MeV). We hope that future experimental investigations will clarify these problems.

6. Acknowledgments

The authors are grateful to L.A. Kondratyuk and A. Matschavariani for useful discussions of the field-theoretic aspects on the vector meson production, H. Matis for providing the DLS filter code and valuable comments, and U. Mosel for correspondence on the Breit-Wigner formula. Two of us (M.I.K. and B.V.M.) are indebted to the Institute for Theoretical Physics of University of Tuebingen for kind hospitality. The work was supported by GSI (Darmstadt) under the contract TÜFÄST, by the Plesler Foundation, and by the Deutsche Forschungsgemeinschaft under the contract No. 436RUS113/367/0(R).

Appendix A. Breit-Wigner description of resonances with energy-dependent widths

Let us consider a process with a resonance in the intermediate state. It can be produced either in a two-body collision or as a result of the decay of a particle or another resonance. Let the resonance further decay to some specific channel i . The amplitude for the total process, \mathcal{M}^i , i.e. the amplitude for resonance production, propagation, and subsequent decay to the channel i is a product of the amplitude of its production \mathcal{M}_p , the resonance propagator, and the amplitude of the resonance decay \mathcal{M}_d^i :

$$\mathcal{M}^i = \mathcal{M}_p \frac{1}{p^2 - m^2 + \Sigma(p^2)} \mathcal{M}_d^i \quad (\text{A.1})$$

where p is the momentum of the resonance, m is its pole mass, $\Sigma(p^2)$ is the resonance self energy. The pole mass m is defined such that $\text{Re}\Sigma(m^2) = 0$. In general, $\text{Re}\Sigma(p^2)$ starts with terms of the order $O((p^2 - m^2)^2)$. These terms are further neglected. The imaginary part of $\Sigma(p^2)$ is equal to

$$\text{Im}\Sigma(p^2) = \frac{1}{2} \sum_i |\mathcal{M}_d^i|^2 \Phi_d^i(p^2) , \quad (\text{A.2})$$

where $\Phi_d^i(p^2)$ is the phase space for the resonance decay into a channel i . We can therefore write either

$$\text{Im}\Sigma(p^2) = \sqrt{p^2} \left(\frac{1}{2\sqrt{p^2}} \sum_i |\mathcal{M}_d^i|^2 \Phi_d^i(p^2) \right) \equiv \sqrt{p^2} \Gamma_{tot}^R(p^2) \quad (\text{A.3})$$

or

$$Im\Sigma(p^2) = m \left(\frac{1}{2m} \sum_i |\mathcal{M}_d^i|^2 \Phi_d^i(p^2) \right) \equiv m \tilde{\Gamma}_{tot}^R(p^2). \quad (\text{A.4})$$

Both definitions of the total width, $\Gamma_{tot}^R(p^2)$ and $\tilde{\Gamma}_{tot}^R(p^2)$, can be used in the relativistic Breit-Wigner formula, but the width should be multiplied by the proper resonance masses, $\sqrt{p^2}$ (running mass) and m (pole mass), respectively. || The square of the amplitude M^i , integrated over the phase space of the final particles with momenta, p_p^k and p_d^l , and normalized by the corresponding factors for the initial particles, gives either a cross section (two initial particles) or a width (one initial particle).

For the scattering problem, the cross section has the form

$$\begin{aligned} d\sigma = & \frac{1}{j2E_12E_2} |\mathcal{M}^i|^2 (2\pi)^4 \delta^{(4)}(p_1 + p_2 - \Sigma_k p_p^k - \Sigma_l p_d^l) \\ & \times \prod_k \frac{d^3 p_p^k}{(2\pi)^3 2E_p^k} \prod_l \frac{d^3 p_d^l}{(2\pi)^3 2E_d^l}, \end{aligned} \quad (\text{A.5})$$

where j is the flux of the incoming particles.

Further, we introduce two δ -functions corresponding to momentum conservation in the processes of production and decay of the resonance and the running mass M of the intermediate resonance

$$\begin{aligned} & \delta^{(4)}(p_1 + p_2 - \Sigma_k p_p^k - \Sigma_l p_d^l) = \\ & = \int \delta^{(4)}(p_1 + p_2 - \Sigma_k p_p^k - p) \delta^{(4)}(p - \Sigma_l p_d^l) d^4 p \int \delta(M^2 - p^2) dM^2 \end{aligned} \quad (\text{A.6})$$

and obtain

$$\sigma = \int \sigma(M^2) \frac{1}{\pi} \frac{M \Gamma_i(M) dM^2}{(M^2 - m^2)^2 + (M \Gamma_{tot}^R(M))^2} \quad (\text{A.7})$$

where

$$M \Gamma_i(M) \equiv m \tilde{\Gamma}_i(M) \equiv \frac{1}{2} |\mathcal{M}_d^i|^2 \Phi_d^i(M^2). \quad (\text{A.8})$$

Here, one should also use the partial widths $\Gamma_i(M)$, $\tilde{\Gamma}_i(M)$ with the proper masses M , m . The similar arguments apply in case of the decay problem.

Appendix B. Effective filter function

A comparison to the DLS data requires to take the experimental detector efficiency into account. For this purpose a filter function is provided by the DLS collaboration. In particular at large T (e.g. $T = 4.88$ GeV) this filter function is not a small correction to the theoretical calculations but is crucial for the comparison to data. Thus, in this appendix we discuss the influence of the detector filter in our analysis.

In terms of the c.m. frame momentum variables, the filter function can be rewritten as

$$f(p_T, y, M) = f(p_T^*, y^* + y_c, M) \quad (\text{B.1})$$

|| In ref.[24] the combination $m_\rho \Gamma_{e^+e^-}^\rho(p^2)$ (physical ρ -meson mass and Γ without " \sim ") has been substituted into the Breit-Wigner formula. Such a combination leads to an additional factor m_ρ/M in the dilepton production cross section and, consequently, to an overestimation of the dilepton yield below the ρ -meson peak. We have brought the attention of the authors of ref.[24] to this circumstance. Recently, a new paper appeared, ref.[25], where that inconsistency has been removed.

where $p_T^* = p_T$ is the transverse momentum of the dilepton pair, y_c is the rapidity of the c.m. frame L^* with respect to the laboratory frame L of the colliding nucleons,

$$y_c = \frac{1}{2} \ln \left(\frac{\sqrt{s} + \sqrt{s - 4m_N^2}}{\sqrt{s} - \sqrt{s - 4m_N^2}} \right), \quad (\text{B.2})$$

T is the proton kinetic energy in the L frame. The distribution of dileptons in the c.m. frame L^* is isotropic. This is a universal feature which does not depend on the specific type of the reactions and is connected to the form of the cross section (4) only. So, we work with the filter function averaged over the angles in the L^* frame:

$$f(p^*, y_c, M) = \int_{-1}^{+1} \frac{d\cos\vartheta}{2} f(p_T^*, y^* + y_c, M) \quad (\text{B.3})$$

where

$$\begin{aligned} p_T^* &= p^* \sin\vartheta, \\ y^* &= \frac{1}{2} \ln \left(\frac{\epsilon^* + p_{||}^*}{\epsilon^* - p_{||}^*} \right), \end{aligned}$$

and

$$\begin{aligned} p_{||}^* &= p^* \cos\vartheta, \\ \epsilon^* &= \sqrt{M^2 + p^{*2}}. \end{aligned}$$

The problem reduces to finding the dilepton distribution over the dilepton momentum p^* in the c.m. frame L^* .

The probability distribution of the dilepton momentum in the L^* frame for the direct decays $V \rightarrow e^+e^-$ is given by

$$dW(p^*) = \sum_{n=0}^{N_\pi} w_n D_n \Phi_2(\sqrt{s}, M, M_X) dM_X^2 \Phi_{2+n}(M_X \dots) \quad (\text{B.4})$$

where

$$\begin{aligned} \Phi_{2+n}(M_X \dots) &= \Phi_{2+n}(M_X, m_N, m_N, \mu_\pi, \dots, \mu_\pi), \\ D_n &= \Phi_{3+n}^{-1}(\sqrt{s}, m_N, m_N, M, \mu_\pi, \dots, \mu_\pi). \end{aligned}$$

The effective filter function can be calculated as follows

$$f^{eff}(T, M) = \sum_{n=0}^{N_\pi} w_n f_n^{eff}(T, M) = \int dW(p^*) f(p^*, y_c, M). \quad (\text{B.5})$$

The value of M_X is integrated out within the limits $2m_N + n\mu_\pi \leq M_X \leq \sqrt{s} - M$. The momentum of the dilepton pair $p^* = p^*(\sqrt{s}, M, M_X)$ is given by

$$p^*(\sqrt{s}, M, M_X) = \frac{\sqrt{(s - (M + M_X)^2)(s - (M - M_X)^2)}}{2\sqrt{s}}.$$

A 100% detector efficiency would yield $f(p_T, y, M) = 1$ and $f^{eff}(T, M) = 1$ in virtue of Eq.(6). The values $f_n^{eff}(T, M)$ are plotted in Fig.5 for the $\rho^0(\omega) \rightarrow e^+e^-$ decays for different values of n at energies $T = 2.09$ and 4.88 GeV.

For the Dalitz decays $\mathcal{M} \rightarrow \mathcal{M}'e^+e^-$, the probability distribution for the dilepton energy ϵ^* in the c.m. frame L^* can be written as follows

$$\begin{aligned} dW(\epsilon^*) &= \sum_{n=0}^{N_\pi} w_n D_n \int_{(2m_N + n\mu_\pi)^2}^{(\sqrt{s} - M)^2} dM_X^2 \int_{-1}^{+1} \frac{d\cos\chi}{2} \delta(\epsilon^* - \eta k) d\epsilon^* \\ &\times \Phi_2(\sqrt{s}, \mu_{\mathcal{M}}, M_X) \Phi_{2+n}(M_X \dots). \end{aligned} \quad (\text{B.6})$$

Here, k is the four momentum of the dilepton pair, $\mu_{\mathcal{M}}$ is the mass of the meson \mathcal{M} in the reaction $pp \rightarrow \mathcal{M}X$ with the subsequent decay $\mathcal{M} \rightarrow \mathcal{M}'e^+e^-$. In the L^* frame, the vector η is defined as $\eta = (1, \mathbf{0})$. The coefficients D_n are defined as before.

Now we should pass to the rest frame L^{**} of the meson \mathcal{M} , where $\eta = \gamma(1, -\mathbf{n}v)$. The γ -factor and the velocity v of the meson \mathcal{M} in the L^* frame are determined by equations

$$\begin{aligned}\gamma\mu_{\mathcal{M}} &= (s + \mu_{\mathcal{M}}^2 - M_X^2)/(2\sqrt{s}), \\ v\gamma\mu_{\mathcal{M}} &= p^*(\sqrt{s}, \mu_{\mathcal{M}}, M_X).\end{aligned}$$

The unit vector \mathbf{n} shows in the direction of the meson velocity in the L^* frame. In the meson rest frame, L^{**} , the dilepton pair has momentum $k = (\epsilon^{**}, \mathbf{n}'p^{**})$ where

$$\begin{aligned}\epsilon^{**} &= (\mu_{\mathcal{M}}^2 + M^2 - \mu_{\mathcal{M}'}^2)/(2\mu_{\mathcal{M}}), \\ p^{**} &= p^*(\mu_{\mathcal{M}}, \mu_{\mathcal{M}'}, M).\end{aligned}$$

The function $p^*(\dots)$ is defined earlier. The unit vector \mathbf{n}' shows in the direction of the dilepton pair momentum in the L^{**} frame. In Eq.(B.6) the value χ is the angle between the directions of the meson velocity in the L^* frame and velocity of the dilepton pair in the L^{**} frame, so that $\cos\chi = \mathbf{n}\mathbf{n}'$ and therefore $\eta k = \gamma(\epsilon^{**}, vp^{**}\cos\chi)$.

In Eq.(40) the integral over the angle χ is evaluated explicitly, and we obtain

$$\frac{dW(\epsilon^*)}{d\epsilon^*} = \sum_{n=0}^{N_{\pi}} w_n D_n \frac{\pi\mu_{\mathcal{M}}}{2\sqrt{sp^{**}}} \int_{(2m_N + n\mu_{\pi})^2}^{(\sqrt{s}-M)^2} dM_X^2 \theta(\epsilon^*, M_X) \Phi_{2+n}(M_X \dots). \quad (\text{B.7})$$

where

$$\theta(\epsilon^*, M_X) = \begin{cases} 1, & \gamma(\epsilon^{**} - vp^{**}) \leq \epsilon^* \leq \gamma(\epsilon^{**} + vp^{**}), \\ 0, & \text{otherwise.} \end{cases} \quad (\text{B.8})$$

The effective filter function can now be calculated to be

$$f_n^{eff}(T, M) = \sum_{n=0}^{N_{\pi}} w_n f_n^{eff}(T, M) = \int dW(\epsilon^*) f(p^*, y_c, M). \quad (\text{B.9})$$

The values $f_n^{eff}(T, M)$ are plotted in Fig.5 for the $\pi^0(\eta) \rightarrow e^+e^-\gamma$ decays for different values of n at energies $T = 2.09$ and 4.88 GeV.

It is now sufficient to multiply the differential cross section (1) with the corresponding effective filter function $f^{eff}(T, M) < 1$ in order to compare the calculations with the experiment. For the evaluation of the direct contributions one should use expression (B.5), while for the Dalitz decays one should use expression (B.9). The function $f^{eff}(T, M)$ is given by a two-dimensional integral in Eq.(B.5) and by a three-dimensional integral in Eq.(B.9).

References

- [1] Walecka J D 1974 *Ann. Phys. (N.Y.)* **83** 491
- [2] Chin S A 1977 *Ann. Phys.* **108** 301
- [3] Drukarev E G and Levin E M 1988 *JETP Lett.* **48** 338
Drukarev E G and Levin E M 1988 *Nucl. Phys.* **A511** 679
- [4] Amadi C and Brown G E 1993 *Phys. Rep.* **234** 1
Hatsuda T, Suomi H, and Kuwabara H, *Progr. Theor. Phys.* **95** 1009
- [5] Mariyama T, Tsushima K and Faessler A 1991 *Nucl. Phys.* **A535** 497
Tsushima K, Maruyama T and Faessler A 1992 *Nucl. Phys.* **A537** 303
- [6] Brown G E and Rho M 1991 *Phys. Rev. Lett.* **66** 2720
- [7] Brown G E and Rho M 1996 *Phys. Rep.* **269** 333
- [8] Agakichiev G *et al* 1995 *Phys. Rev. Lett.* **75** 1272
Drees A 1996 *Nucl. Phys.* **A610** 536c
- [9] Masera M 1995 *Nucl. Phys.* **A590** 93c
- [10] Porter R J *et al* 1997 *Phys. Rev. Lett.* **79** 1229
- [11] Bianchi N *et al* 1993 *Phys. Lett.* **B309** 5
Bianchi N *et al* 1993 *Phys. Lett.* **B325** 333
- [12] Kondratyuk L A, Krivoruchenko M I, Bianchi N, De Sanctis E and Muccifora V 1994 *Nucl. Phys.* **A579** 453
- [13] Weisskopf V 1993 *Physikalische Zeitschrift* **34** 1
- [14] Sobelman I I 1972 *Introduction to the Theory of Atomic Spectra*, Pergamon Press, Oxford *e a*
- [15] Koch P 1992 *Phys. Lett.* **B228** 187
- [16] Li G Q, Ko C M, Brown G E 1995 *Phys. Rev. Lett.* **75** 4007
- [17] Cassing W, Ehehalt W and Kralik L 1996 *Phys. Lett.* **B377** 5
- [18] Rapp R, Chanfray G and Wambach J 1997 *Nucl. Phys.* **A617** (1997) 472
- [19] Peters W, Post M, Lenske H, Leupold S and Mosel U 1998 *Nucl. Phys.* **A632** 109
- [20] Bratkovskaya E L and Ko C M 1999 *Phys. Lett.* **B445** 265
- [21] Friese J for the HADES Collaboration 1999 *Prog. Part. Nucl. Phys.* **42** 235
- [22] Wilson W K *et al* 1998 *Phys. Rev.* **C57** 1865
- [23] Ernst C, Bass S A, Belkacem M, Stocker H and Greiner W 1998 *Phys. Rev. C* **58** 447
- [24] Bratkovskaya E L, Cassing W, Effenberger M and Mosel U 1999 *Nucl. Phys.* **A653** 301
- [25] Bratkovskaya E L, Cassing W and Mosel U 2001 *Nucl. Phys.* **A686** 568
- [26] Alexander G *et al* 1967 *Phys. Rev.* **154** 1284
- [27] Calen H *et al* 1996 *Phys. Lett.* **B366** 39
Flaminio V, Moorhead W G, Morrison D R O and Rivoire N 1984 *Preprint CERN-HERA-84-01* (unpublished)
- [28] Chiavassa E *et al* 1994 *Phys. Lett.* **B337** 192
- [29] Alexander G 1967 *et al* 1967 *Phys. Rev.* **154** 1284
Bystricky J and Lehar F 1981 *Nucleon-Nucleon Scattering Data; Physics Data*, edited by H. Behrens and G. Ebel (Fachinformationszentrum, Karlsruhe), Nos. 11-2 and 11-3
Shimizu F *et al* 1982 *Nucl. Phys.* **A386** 571
Dakhno L G *et al* 1983 *Yad. Fiz.* **37** 907
Baldini A, Flaminio V, Moorhead W G and Morrison D R O 1988 *Total Cross-Sections for Reactions of High Energy Particles (Including Elastic, Topological, Inclusive and Exclusive Reactions)*, edited by H. Schopper, *Landolt-Bornstein*, Vol. I/12, Springer, Berlin.
- [30] Ganhyug B 1998 *Description of π -Meson and Proton Characteristics in np-Interactions at $P_n = 1.25 - 5.1$ GeV/c within the framework of FRITIOF Model*, Preprint P2-98-26, Laboratory of High Energies, JINR, Dubna
- [31] Haglin K and Gale C 1993 *Phys. Rev.* **C49** 401
- [32] Baatar Ts *et al* 1999 *An Analysis of Characteristics for π - Mesons and Protons in Inelastic AC-Interactions at $p = 4.2$ GeV/c per Nucleon in the framework of FRITIOF Model* Preprint P1-99-45, Laboratory of High Energies, JINR, Dubna
- [33] Ganhyug B 1998 *Description of π -Meson and Proton Characteristics in np-Interactions at $P_n = 1.25 - 5.1$ GeV/c within the framework of FRITIOF Model*, Preprint P2-98-26, Laboratory of High Energies, JINR, Dubna
- [34] Beshliu K *et al* *Yad. Fiz.* **43** 888
- [35] Faessler A, Fuchs C and Krivoruchenko M I 2000 *Phys. Rev.* **C61** 035206
- [36] Kroll N M, Lee T D and Zumino B 1967 *Phys. Rev.* **157** 1376
- [37] Krivoruchenko M I and Faessler A 2002 *Phys. Rev.* **D65** 017502

- [38] Krivoruchenko M I, Martemyanov B V, Faessler A and Fuchs C 2002 *Ann. Phys. (N.Y.)* **296** 100
- [39] Shechter K, Faessler A, Fuchs C, Krivoruchenko M I and Martemyanov B V, in preparation.
- [40] Matveev V A, Muradyan R M and Tavkhelidze A N 1973 *Lett. Nuovo Cim.* **7** 719
Brodsky S J and Farrar G R 1973 *Phys. Rev. Lett.* **31** 1153
Brodsky S J and Farrar G R 1975 *Phys. Rev. D* **11** 1309
- [41] Vainstein A I and Zakharov V I 1978 *Phys. Lett.* **B72** 368
- [42] Jones H F and Scadron M D 1973 *Ann. Phys. (N.Y.)* **81** 1
- [43] Devenish R C E, Eisenschitz T S and Körner J G 1976 *Phys. Rev. D* **14** 3063
- [44] Trueman T L 1969 *Phys. Rev.* **182** 1469
Theis W R and Hertel P 1970 *Nuovo. Cim.* **66** 152
Close F E and Cottingham W N 1975 *Nucl. Phys.* **B99** 61
Bardin W A and Tung Wu-Ki 1968 *Phys. Rev.* **173** 1423
Tarrach R 1975 *Nuovo Cim.* **A28** 409
- [45] Koniuk R 1982 *Nucl. Phys.* **B195** 452
Capstick S and Roberts S 1994 *Phys. Rev. D* **49** 4570
Stassart P and Stancu F 1990 *Phys. Rev. D* **42** 1521
Stancu F and Stassart P 1993 *Phys. Rev. D* **47** 2140
- [46] Manley P and Saleski E M 1992 *Phys. Rev. D* **45** 4002